

March 15, 1990

Ferromagnetic-resonance of single-crystal YIG/ gadolinium gallium garnet/YIG layers

K. Sun

C. Vittoria
Northeastern University

H. L. Glass

P. Degasperis

R. Marcelli

Recommended Citation

Sun, K.; Vittoria, C.; Glass, H. L.; Degasperis, P.; and Marcelli, R., "Ferromagnetic-resonance of single-crystal YIG/gadolinium gallium garnet/YIG layers" (1990). *Electrical and Computer Engineering Faculty Publications*. Paper 51. <http://hdl.handle.net/2047/d20002222>



Ferromagnetic resonance of singlecrystal YIG/gadolinium gallium garnet/YIG layers

Kunquan Sun, Carmine Vittoria, H. L. Glass, P. De Gasperis, and R. Marcelli

Citation: *J. Appl. Phys.* **67**, 3088 (1990); doi: 10.1063/1.345383

View online: <http://dx.doi.org/10.1063/1.345383>

View Table of Contents: <http://jap.aip.org/resource/1/JAPIAU/v67/i6>

Published by the [American Institute of Physics](#).

Related Articles

Evolution of ferromagnetic and spin-wave resonances with crystalline order in thin films of full-Heusler alloy Co₂MnSi

J. Appl. Phys. **111**, 023912 (2012)

Frequency-selective control of ferromagnetic resonance linewidth in magnetic multilayers

Appl. Phys. Lett. **100**, 032402 (2012)

Spin wave modes in ferromagnetic tubes

J. Appl. Phys. **111**, 013905 (2012)

Hysteretic spin-wave excitation in spin-torque oscillators as a function of the in-plane field angle: A micromagnetic description

J. Appl. Phys. **110**, 123913 (2011)

Multi-domain resonance in textured Z-type hexagonal ferrite

J. Appl. Phys. **110**, 123901 (2011)

Additional information on *J. Appl. Phys.*

Journal Homepage: <http://jap.aip.org/>

Journal Information: http://jap.aip.org/about/about_the_journal

Top downloads: http://jap.aip.org/features/most_downloaded

Information for Authors: <http://jap.aip.org/authors>

ADVERTISEMENT

LakeShore Model 8404 developed with **TOYO Corporation**
NEW AC/DC Hall Effect System Measure mobilities down to 0.001 cm²/V s

Ferromagnetic resonance of single-crystal YIG/gadolinium gallium garnet/YIG layers

Kunquan Sun and Carmine Vittoria

Department of Electrical and Computer Engineering, Northeastern University, Boston, Massachusetts 02115

H. L. Glass

Science Center-Rockwell International, Anaheim, California 92803

P. De Gasperis and R. Marcelli

Istituto di Elettronica dello Stato Solido del CNR, Via Cineto Romano 42, 00156 Roma, Italy

We report on the microwave properties of single-crystal YIG/gadolinium gallium garnet/YIG grown in (110) layers, where YIG is yttrium iron garnet. The YIG layers were sufficiently thin so that single domain ferromagnetic resonance (FMR) was observed. FMR fields were measured as a function of field direction and magnitude and frequency. Bulk magnetic parameters deduced from FMR and vibrating-sample magnetometer measurements agree with published values. In addition, FMR measurements at low fields show typical "butterfly" variations of the FMR fields with a frequency for H , the magnetic field, parallel to either the $\langle 100 \rangle$ or $\langle 110 \rangle$ axis. However, a new butterfly pattern was also observed for the magnetic field parallel to the $\langle 111 \rangle$ axis. This result is intrinsic to layered structures and not to single layer excitations. We attribute this new result to nonuniform distribution of strain in the two YIG layers, and as a consequence, we predict that magnetostatic fringe fields from edges are sufficient to induce spin-flop magnetic configurations in single-crystal YIG double layers.

I. INTRODUCTION

Due to the successful production of magnetic multilayered structures, there has recently been considerable interest¹⁻³ in the microwave properties of magnetic multilayered structures. In particular, the study of double layered structures are of special interest, since it is the simplest structure to consider from a production point of view as well as understanding its physical properties. Besides the study of fundamental properties of such structures there are many applications that are unique to double layers. For example, magnetostatic wave propagation in double layered structures of YIG yields a higher bandwidth⁴ of operation in comparison to single layer.

In this paper we report on the microwave resonance properties of a single-crystal layered structure of YIG/GGG/YIG/GGG. The film planes were purposely chosen to be the (110) planes so that the easy axis of magnetization in each YIG layer was in the film plane. Thus, in zero magnetic field the magnetization in an idealized YIG layer is parallel to the $\langle 111 \rangle$ axis. This implies that the magnetization in each layer is parallel to each other at zero field. However, minimization of free energy implies that the magnetization in each layer is antiparallel. Thus, the purpose of this work was to initiate a microwave characterization study involving two magnetic materials in which spin flop can be induced in zero field with the total magnetization equal to zero. We approached this research with the expectation that ferromagnetic resonance properties of a two layered structure would be different from the single layer case at low fields.

Experimentally we find that for zero magnetic field the total saturation magnetization is only reduced by approximately 10% from the maximum saturated value in high ex-

tended magnetic fields. However, as we reversed the applied field along the $\langle 111 \rangle$ axis, we find indeed that zero total magnetization (spin-flop condition) is obtained for $H = -2$ Oe. The FMR frequency as a function of H (along the $\langle 111 \rangle$ axis) exhibited a butterfly pattern that contrasted with single layer results. We attribute this microwave resonance result in terms of a different strain distribution in each layer. As a result the static magnetization in each layer of the double layered structure is not collinear due to H_u (uniaxial anisotropy field) being different in each layer. The misalignment of the two magnetizations depends on H_u as well as H . Reasonable agreement between FMR experimental results and calculation was obtained, in which both cubic anisotropy field (H_A) and H_u , H , g , and $4\pi M$ were included in the theoretical formulation. In our model H_u was the only parameter to be allowed to vary from layer to layer, since the two films are expected to be strained differently by the substrate.

II. RESULTS

A. In-plane angular variation of the FMR of field

The geometry of the two layered structure is shown in Fig. 1. The two magnetizations of the two YIG layers are represented by M_1 and M_2 , respectively. H_a is the applied magnetic dc field. In Fig. 2, the capital letters refer to the crystal axes while (ϕ, β) , (ϕ_1, θ_1) , and (ϕ_2, θ_2) refer to the angular distributions of H_a , M_1 , and M_2 , respectively. The thickness of the sample is $d_1 + d_2 + d_3 + d_4$, where d_1 and d_3 represent the thicknesses of layer 1 (M_1) and layer 2 (M_2), d_2 ($1 \mu\text{m}$) is the thickness of paramagnetic GGG film between the two YIG films and d_4 is far greater than $d_1 + d_2 + d_3$ and is the thickness of the substrate. The diam-

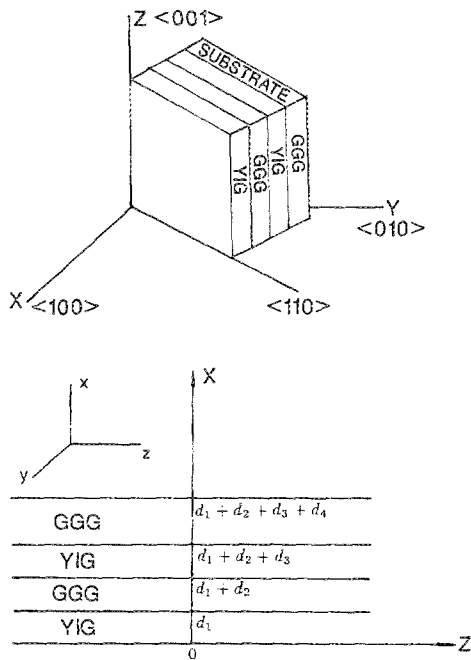


FIG. 1. Cross view of the geometrical configuration of the double layered YIG film.

eter of the sample was 5 mm.

The ferromagnetic resonance (FMR) technique was used to measure the in-plane anisotropy field of each YIG film in the layered structure. The sample was placed at the center of a microwave cavity excited in a rectangular TE_{102}

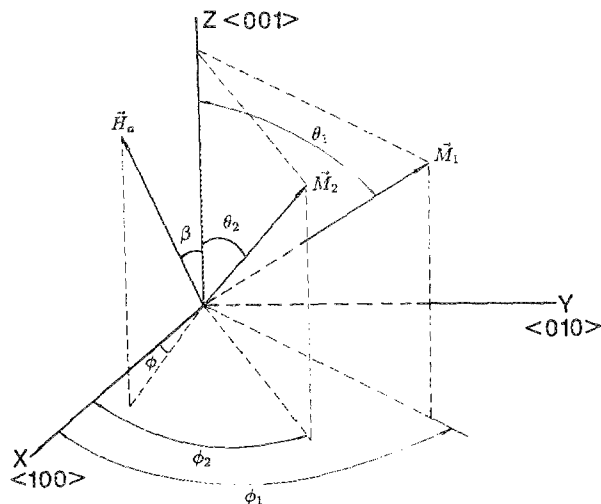


FIG. 2. Orientation of the double layered YIG film in relation to the angular parameters used for the calculations. The capital letters refer to the crystal axes while (ϕ, β) , (ϕ_1, θ_1) , and (ϕ_2, θ_2) refer to the angular distributions of \vec{H}_a , \vec{M}_1 , and \vec{M}_2 .

mode. The static magnetic field \vec{H}_a was applied in the plane of the film and the rf field was normal to the plane of the film. The sample was rotated with an axis of rotation normal to the film plane and the applied dc field direction was fixed in direction.

In order to determine bulk parameters of the layered films, the FMR field H_r was plotted as a function of the angle β between the applied field \vec{H}_a and the $\langle 100 \rangle$ axis, see Fig. 3. It is noted in Fig. 3 that there exist two resonant curves, each of which corresponds to one layer of the single-crystal double layer film. In order to attribute each resonance to its corresponding YIG layer the top layer was mechanically polished. After each polishing step the FMR signal was recorded and compared with previous FMR results. A decrease in the magnitude of the resonant signal was attributed to the thinning of the YIG layer exposed to the free surface. As indicated in Fig. 3, for a fixed value of ω , the higher resonant magnetic field is associated with the layer exposed to air while the lower one is associated with the layer between the two GGG layers. The amplitude of the FMR signal corresponding to the top layer is larger than that of the bottom layer. The effect of the uniaxial anisotropy field in the top layer is to shift the minimum resonant field (H_r) vs β towards the $[001]$ axis relative to the bottom layer, where the easy axis of magnetization for the uniaxial magnetic anisotropy energy is the $\langle 100 \rangle$ axis. The direction of \vec{M}_2 is no longer 54.6° relative to the $[001]$ axis for the top layer due to the induced in-plane anisotropy field. From Fig. 3, it is found that β_{\min} for the top layer is about 45° .

The data was fitted to a calculation of H_r based upon the total free magnetic potential energy of the layered structure. The free magnetic potential energy of the whole structure is the sum of the free energy of each individual layer,

$$F = F_1 + F_2. \quad (1)$$

For the case of \vec{H} in the $(1\bar{1}0)$ plane, the free potential energy of each layer is given^{5,6} as

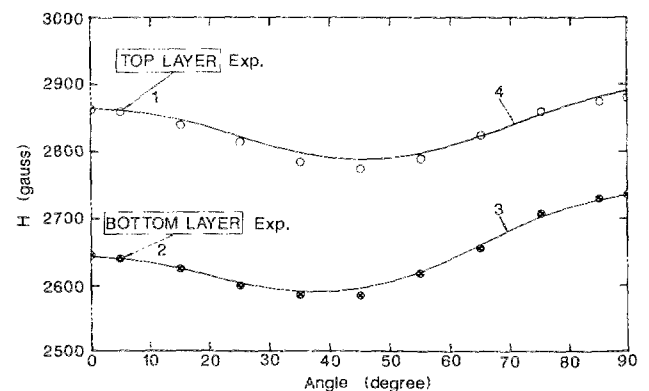


FIG. 3. Magnetic resonant field vs the angle between \vec{H} and the $[001]$ axis. (1) Exp. (top layer); (2) Exp. (bottom layer); (3) Theory, $4\pi M_{\text{eff}} = 1750 \text{ G}$, $2K_u^{(1)}/M_{\text{eff}} = -82 \text{ Oe}$, $2K_v^{(1)}/M_{\text{eff}} = 0$; (4) Theory, $4\pi M_{\text{eff}} = 1256 \text{ G}$, $2K_u^{(2)}/M_{\text{eff}} = -82 \text{ Oe}$, $2K_v^{(2)}/M_{\text{eff}} = 50 \text{ Oe}$.

$$F_i = -HM_i[\cos\theta_i\cos\beta + \sin\theta_i\sin\beta\cos(\phi_i - \pi/4)] + \pi M_i^2[\sin^2\theta_i(1 - \sin 2\theta_i)] + K_i^{(i)}[(3 - 4\cos 2\theta_i + \cos 4\theta_i)(1 - \cos 4\theta_i)/8 + 1 - \cos 4\theta_i]/8 - K_u^{(i)}\cos^2(\theta_i - \alpha_i), \quad i = 1, 2, \quad (2)$$

where θ_i and ϕ_i are the polar and azimuthal angles of M_i and α_i is the angle between the easy axis of the in-plane anisotropy and the [001] axis. In Eq. (2) the magnetizing, demagnetizing, cubic anisotropy $K_i^{(i)}$, and the in-plane induced anisotropy $K_u^{(i)}$ energies are included. $i = 1, 2$ denotes the corresponding parameters for layers 1 and 2.

From equilibrium conditions we obtain

$$\frac{\partial F}{\partial \theta_i} = 0, \quad i = 1, 2, \quad (3)$$

$$\frac{\partial F}{\partial \phi_i} = 0, \quad i = 1, 2. \quad (4)$$

Thus, we have $\phi_i = 45^\circ$, $i = 1, 2$ and

$$(\omega_i/\gamma)^2 = [HM_i \sin\beta \sin\theta_{i0} - K_i^{(i)}(\cos 4\theta_{i0} - 4\cos 2\theta_{i0} + 3)/4 + 4\pi M_i^2 \sin^2\theta_{i0}] \times [HM_i \cos(\theta_{i0} - \beta) + K_i^{(i)}(3\cos 4\theta_{i0} + \cos 2\theta_{i0}/2 + 2K_u^{(i)}\cos 2(\theta_{i0} - \alpha_i))/M_i^2 \sin^2\theta_{i0}], \quad i = 1, 2. \quad (7)$$

In Fig. 3 the experimental curves and data fitting curves for the FMR field H_r vs β at 9.5 GHz are shown. The following parameters were deduced from the fit. For the layer next to the GGG substrate (layer 1), we have $4\pi M_{\text{eff}}^{(1)} = 1750$ G, $2K_1^{(1)}/M = -82$ Oe, $2K_u^{(1)}/M = 0$. For the other layer (layer 2) we have $4\pi M_{\text{eff}}^{(2)} = 1256$ G, $2K_1^{(2)}/M = -82$ Oe, $2K_u^{(2)}/M = 50$ Oe, and $g = 2.025$, where $4\pi M_{\text{eff}}^{(i)}$ ($i = 1, 2$) is the sum of the saturation magnetization and any source of uniaxial magnetic anisotropy field *normal* to the film plane.

In order to maximize the effect of substrate lattice mismatch on the direction of M in the film plane, YIG films were grown on {110} substrates of GGG. With no strain one would naturally expect M to be parallel to the $\langle 111 \rangle$ axis in each YIG layer. However, the lattice mismatch between substrate and a given layer induces⁷ a strain or a uniaxial anisotropy field H_u in the film plane as well as perpendicular to the {110} plane. The effect of H_u is to rotate M away from the $\langle 111 \rangle$ axis, toward the $\langle 100 \rangle$ axis. Hence, if the layers are strained, M is not necessarily parallel to the $\langle 111 \rangle$ axis or to each other in the two films. Interestingly, films grown in the {100} plane do not induce any uniaxial field in the film plane even if the films are strained.

B. Frequency swept FMR experiments

A similar experiment was carried out by putting the sample at the junction of a slot-co-planar device⁸ to measure the resonant frequency for fixed magnetic field amplitude. In this experiment, the frequency is swept while H is fixed. For experiments in part A, the field is swept while the frequency is fixed at 9.5 GHz. In the slotline measurements in which the frequency is swept and the applied field is parallel to the $\langle 111 \rangle$ axis, the measured FMR frequency versus H shows, Fig. 4(a), that neither layer exhibits linearity between fre-

$$HM_i \sin(\beta - \theta_i) = [K_1^{(i)}/4 + K_u^{(i)}] \sin 2\theta_i + (3K_1^{(i)}/8) \sin 4\theta_i, \quad i = 1, 2. \quad (5)$$

The equilibrium angle $\phi_i = 45^\circ$ means that both M_1 and M_2 lie in the film plane for all angles of $H(\beta)$ in the plane (see Fig. 2). Resonant conditions are calculated from

$$\left(\frac{\omega_i}{\gamma}\right)^2 = \frac{1}{M_i^2 \sin^2\theta_i} \left[\frac{\partial^2 F}{\partial \theta_i^2} \frac{\partial^2 F}{\partial \phi_i^2} - \left(\frac{\partial^2 F}{\partial \theta_i \partial \phi_i}\right)^2 \right]_{\theta_i = \theta_{i0}, \phi_i = \phi_{i0}}, \quad i = 1, 2, \quad (6)$$

where $\gamma = g(e/2mc)$, θ_{i0} and ϕ_{i0} are the equilibrium angles at resonance, $\omega_i/2\pi$ is the operating frequency. Substituting Eq. (1) into (6) yields

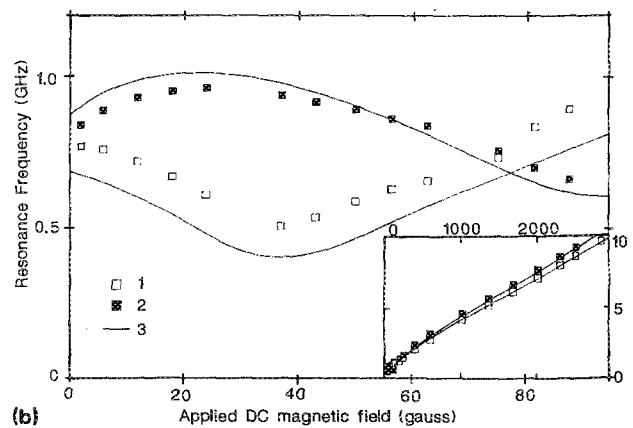
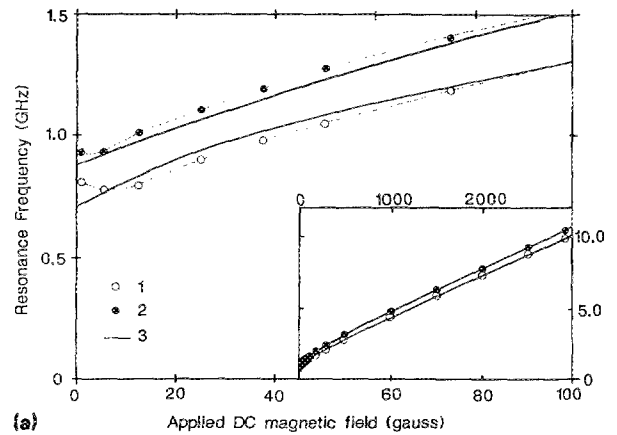


FIG. 4. (a) Resonant frequency as a function of static magnetic field for the applied magnetic field along the $\langle 111 \rangle$ axis. (1) Exp. (top layer); (2) Exp. (bottom layer); (3) Theory. (b) Resonant frequency as a function of static magnetic field for the applied magnetic field along the $\langle 100 \rangle$ axis. (1) Exp. (top layer); (2) Exp. (bottom layer); (3) Theory.

quency and H at low fields. The FMR frequencies for both layers reach minimum values when the applied magnetic field is directed along the $\langle 111 \rangle$ axis and is approximately equal to 5 G. The data for H along the $\langle 100 \rangle$ axis are shown in Fig. 4(b) and it is found that the data is in reasonable agreement with the calculations contained in part A. Using parameters deduced from the angular variation experiment at 9.5 GHz (part A) we were able to fit the data for frequency versus H in the case of H directed along the $\langle 110 \rangle$ and $\langle 100 \rangle$ axes. For H parallel to the $\langle 111 \rangle$ axis we had to modify our calculations in order to fit the low-field data.

Due to the uniaxial anisotropy field (H_u) being different at each layer, the static magnetization direction in each layer is directed differently with respect to each other, especially in zero magnetic field. In our case, the induced in-plane anisotropy energy K_u is not zero for layer 2 (M_2) while K_u is zero for layer 1 (M_1). So M_1 is directed along the $\langle 111 \rangle$ cubic axis, that is, $\theta_{10} = 54.6^\circ$. M_2 lies between the $\langle 111 \rangle$ and $\langle 100 \rangle$ cubic axes, since H_u is not zero. In fact, this finding is confirmed in the FMR experiment, Fig. 4(a), and in the vibrating-sample magnetometer (VSM) measurement, Fig. 5. For example, in Fig. 4(a), if we substitute ω and the corresponding FMR field from the branch labeled top layer into Eq. (7), one may determine θ_2 uniquely. Similarly, for the other branch labeled bottom layer, θ_1 may also be calculable in the same manner. Thus, for any value of H , including zero, the misalignment between M_1 and M_2 may be obtained by simply taking the result of $\theta_2 - \theta_1$. This difference is plotted in Fig. 6. In essence, there were no adjustable parameters in fitting the data for H near zero field. In order to obtain a realistic comparison between measured and calculated FMR field near $H \approx 0$. We measured $\theta_2 - \theta_1 = \alpha$ indirectly from VSM techniques. The hysteresis loop for magnetization was measured for H along the easy axis $\langle 111 \rangle$. The angle between the two static magnetizations was determined by using $(M + M \cos \alpha)/2M = R$, where M is the saturation magnetization, α is the angle between the two static magnetizations, and R is the ratio of the magnetization with field versus the saturated magnetization from the hysteresis loop. The angle α deduced from FMR data decreases with H faster than that determined from VSM data. How-

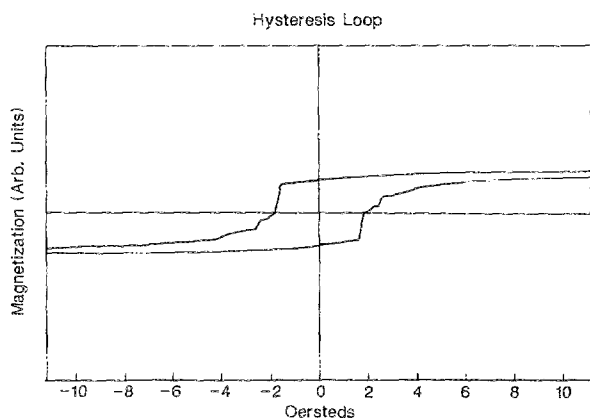


FIG. 5. Hysteresis loop of the double layered YIG film along the easy axis ($\langle 111 \rangle$ axis).

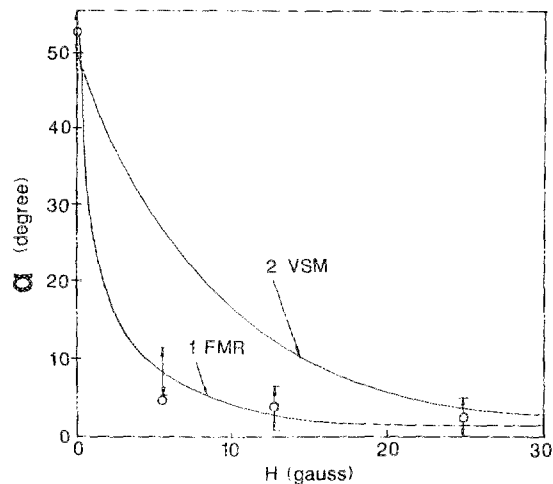


FIG. 6. Angle between the two static magnetizations vs the applied dc magnetic field. (1) Exp. (from VSM data); (2) Exp. (from FMR data).

ever, α obtained from both sets of data are in qualitative agreement. Reasonable fit is obtained to the FMR data for H parallel to the $\langle 111 \rangle$ cubic axis in low fields, if we assume α determined from the VSM data.

In summary, in zero magnetic field we have estimated from the equilibrium conditions [Eq. (7)] that the angle between M_1 and M_2 is 24° ; the VSM and FMR data implies that this angle is about 50° . We conclude that the effect of the fringe fields is to increase the angle between M_1 and M_2 in a manner to prefer antialignment between M_1 and M_2 . This is reasonable in view of the fact that a spin flop (180° between M_1 and M_2) was obtained in a reversed field of 2 Oe (see Fig. 5). In the spin-flop configuration it is well known that the magnetostatic fringe field between layers is minimized.

C. Spin-wave resonance experiments

In another FMR experiment the dc magnetic field was applied normal to the $\{110\}$ plane in order to obtain spin-wave dispersions at 9.5 GHz. The spin-wave dispersions for the two different YIG layers are shown in Figs. 7(a) and 7(b). The thicknesses of the two YIG layers were determined by

$$\frac{\omega_i}{\gamma} = H_{\text{ext}} - 4\pi M_{\text{eff}}^{(i)} + \frac{2A}{M} \frac{\pi^2}{d_i^2} n^2,$$

where $A = 0.473 \times 10^{-6}$ ergs/cm, H_{ext} is the external field, d_i is the thickness of the film, and n denotes the order of the spin-wave modes. It is found that for layer 1 $d_1 = 0.88 \mu\text{m}$ and for layer 2 $d_2 = 0.94 \mu\text{m}$, which is consistent with optical interference measurements of d_1 and d_2 . The difference here is that we were able to identify the thickness to correspond to a particular layer within the layered structure.

III. CONCLUSIONS

FMR and VSM measurements were performed on single-crystal double-layered YIG film. For low or zero fields, the two static magnetizations in the two YIG layers are not collinear. The angle between the two magnetizations has a

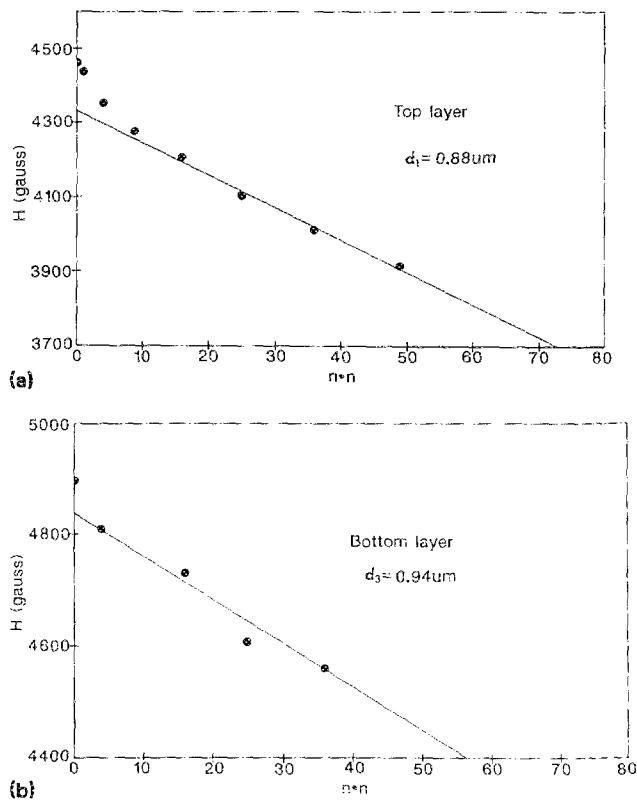


FIG. 7. (a) Spin-wave dispersion for the top layer. (b) Spin-wave dispersion for the bottom layer.

strong affect on FMR frequencies for low applied magnetic fields. The misalignment between the two magnetizations is caused by the uniaxial anisotropy field induced in one of the two layers. Undoubtedly, strain between film and substrate

is the main source for the uniaxial anisotropy field. We determined, in particular, that $H_u = -50$ Oe in layer 2 and $H_u = 0$ in layer 1. As a consequence, in zero field M_1 is directed along the $\langle 111 \rangle$ axis while M_2 is rotated towards the $\langle 100 \rangle$ axis and away from the $\langle 111 \rangle$ axis. The misalignment between M_1 and M_2 depends on the uniaxial anisotropy field and the applied field as well as the fringe field. The misalignment reaches a maximum angle of 180° for $H = -2$ Oe. It is clear that total free energy models based solely on single layer free energies will not be sufficient to explain FMR data in layered structures near zero field. In particular, the spin-flop condition should be explored in the future at microwave frequencies, since it is a unique property of layered structures.

ACKNOWLEDGMENTS

The authors wish to thank the Office of Naval Research for supporting the research in part. We also want to thank V. Harris for his help in the experiment.

¹S. McNight and C. Vittoria, Phys. Rev. B **36**, 8574 (1987).

²R. E. Camley, Phys. Rev. B **27**, 261 (1983).

³P. Grünberg and K. Mika, Phys. Rev. B **27**, 2955 (1983).

⁴A. K. Ganguly and C. Vittoria, J. Appl. Phys. **45**, 4665 (1974).

⁵J. O. Artman, Phys. Rev. **105**, 74 (1957).

⁶C. Vittoria, H. Lessoff, and N. D. Wilsey, IEEE Trans. Magn. **MAG-8**, 273 (1972).

⁷J. E. Mee, G. R. Pulliam, J. L. Archer, and P. J. Besser, IEEE Trans. Magn. **MAG-5**, 717 (1969).

⁸K. Sun, Y. Liu, and C. Vittoria, Progress In Electromagnetics Research Symposium, p. 249 (1989).